Reviews in Plasmonics

Chris D. Geddes *Editor*

Reviews in Plasmonics 2010

Springer

Reviews in Plasmonics

Editor
Chris D. Geddes, Ph.D., CSci, CPhys, CChem, MIoP, MRSC

For further volumes:
http://www.springer.com/series/7164

Chris D. Geddes
Editor

Reviews in Plasmonics 2010

Springer

Editor
Chris D. Geddes
University of Maryland
Baltimore County, MD 21202, USA
geddes@umbc.edu

ISSN 1573-8086
ISBN 978-1-4614-0883-3 e-ISBN 978-1-4614-0884-0
DOI 10.1007/978-1-4614-0884-0
Springer New York Dordrecht Heidelberg London

Library of Congress Control Number: 2011941008

Preface

In the last 10 years, we have seen significant growth in plasmonics-related research with many researchers around the world publishing high quality material in now several peer reviewed journals, solely dedicated to the topic. To this end, we launched the "*Plasmonics*" Springer journal in 2005, which after only a few years, now has an ISI impact factor close to 4. This rapid growth of the journal in this area of science reflects the need for plasmonics-based publishing media. To address this ever-growing need, we are now launching a new hard bound review volume, "*Reviews in Plasmonics*," which is solely dedicated to publishing review articles, which are typically considered too lengthy for journal publication.

In this first volume, we have invited notable scientists from around the world to review their findings, including works on nanoparticle synthesis, SPR-based sensors, SERS as well as plasmon-assisted fluorescence, typically referred to as metal-enhanced fluorescence, to name but just a few. We subsequently thank the authors for their most timely and notable contributions and we all hope you find this volume a useful resource.

Finally, we would like to thank Caroleann Aitken, the Institute of Fluorescence manager, for helping compile the volume, as well as Michael Weston of Springer for help in launching the volume.

Baltimore, MD, USA — Dr. Chris D. Geddes, Professor

Contents

Chapter 1
Metal Nanoparticles for Molecular Plasmonics

Andrea Steinbrück, Andrea Csaki, and Wolfgang Fritzsche

1 Introduction

The color induced by metal nanoparticles has attracted people's attention since hundreds of years. Probably, the most famous example for the use of gold nanoparticles for staining is the Lycurgus Cup that was manufactured in the fifth to fourth century BC. This probably accidental application was later extended to a more controlled technique for coloring glass, today still visible in many colorful church windows. A global summary of the historical approaches, especially for gold colloids can be found elsewhere [35]. Michael Faraday (1791–1867) and Gustav Mie (1869–1957) were the most famous scientists who laid the systematic groundwork for synthesis and theoretical calculations of colloidal solutions. Faraday synthesized gold nanoparticles in 1857 and called them "activated gold" [47]. Shortly after that, Graham established the term "colloid" [67]. The theoretical calculations for metal nanoparticles of Mie [142] are still used today by many scientists. Mie worked on the issue of light scattering by small spheres of arbitrary size and material, and calculated the response of such a metal sphere to an external electromagnetic field (light). The Mie theory is based on the solution of Maxwell's equations for (subwavelength-sized) spheres in a nonabsorbing medium. The most important free parameter is the sphere radius. Material properties are considered as frequency-dependent permittivity. Another important fact is that the Mie theory is true only for uncharged spherical particles. It should be mentioned that almost at the same time Debye solved the same

A. Steinbrück
Nano Biophotonics Department, Institute of Photonic Technology,
PO Box 100239, Jena 07702, Germany

Chemistry Division, Los Alamos National Laboratory, Los Alamos, NM 87545, USA

A. Csaki • W. Fritzsche (✉)
Nano Biophotonics Department, Institute of Photonic Technology,
PO Box 100239, Jena 07702, Germany
e-mail: fritzsche@ipht-jena.de

C.D. Geddes (ed.), *Reviews in Plasmonics 2010*, Reviews in Plasmonics,
DOI 10.1007/978-1-4614-0884-0_1, © Springer Science+Business Media, LLC 2012

problem too [36]. Furthermore, since the interest grew for investigations of nanoparticles with variable shape or for bimetallic particles, several models or approximations were calculated by other scientists as well [100] and [116].

As already mentioned, the color of colloidal solutions is an eye-catching property. This color is explained as the result of a collective oscillation of electrons of the conductive electron band near the Fermi level. This effect causes a so-called localized (surface) plasmon (LSP) band in the spectra where absorption reaches a maximum at a certain wavelength of light. The location of the LSP band is characteristic for the material, the size, the shape, and the surrounding medium of a nanoparticle. The size distribution is so mirrored in the spectrum. A narrow size distribution causes a sharp LSP band, whereas a wide distribution reflects in a broad absorption band. In bimetallic particles, the location of the LSP band(s) depends further on the composition and the distribution of the two metals [116].

Only metals with free electrons (Au, Ag, Cu) possess plasmon resonances in the visible spectrum and therefore intense colors. The shape of the particles influences these resonances, as, e.g., elongated nanoparticles (rods) display two distinct plasmon bands related to transverse and longitudinal electron oscillations. The longitudinal oscillation is very sensitive to the aspect ratio of the particles [129].

A growing interest in the optical properties of the nanoparticles is supported by the need for enhanced bioanalytical methods. The potential of surface plasmon resonance in this field was demonstrated by the impressive technical development for bioanalytical applications based on surface plasmon resonance on thin metal layers [107]. This trend is supported by the progress in the controlled synthesis as well as sophisticated bioconjugation of metal nanoparticles in combination with molecular principles; and opened a new field for nanoparticle-based molecular nanotechnology [55]. In addition, the impetus for understanding the mechanisms of optical processes in nanoscale systems represents another strong motivation for work in molecular plasmonics, as this interdisciplinary field between nanoparticle plasmonics and molecular construction is dubbed. This review intends to give an overview about nanoparticle synthesis and related optical properties, as well as about the state of the art of bioconjugation of nanoparticles in order to realize molecular constructs for potential applications.

2 Synthesis of Nanoparticles

Since the days of Faraday, the synthesis of nanoparticles has made substantial progress. Today, people have succeeded to synthesize stable nanoparticles with variable sizes (but a sharp size distribution), shapes, and materials by reliable procedures. Nanoparticles can be produced of many metals such as Au, Ag, Cu, Pt, Pd, Ru, and others. The principles of the synthesis process of nanoparticles have been investigated and are yet much better understood even though there are some questions left to answer. For the characterization of nanoparticles, several methods are used. Transmission electron microscopy (TEM), high-resolution TEM (HRTEM), atomic

force microscopy (AFM), scanning electron microscopy (SEM), X-ray diffraction, and other methods image the size, shape, and ultrastructure of the particles; UV–vis spectroscopy is applied to analyze their optical properties.

2.1 Materials

2.1.1 Gold Nanoparticles

Schmid and coworkers did pioneering work on well-defined phosphine-stabilized gold clusters [178, 181]. The gold clusters they had synthesized had the size of about 1.4 nm with a narrow size distribution. This work contributed remarkably to the understanding of the properties of small metal particles.

A currently very common method for the synthesis of gold nanoparticles was introduced by Turkevich [207]. He produced 20 nm gold nanoparticles by citrate reduction of $HAuCl_4$ in water. Frens succeeded in the preparation of gold nanoparticles with variable sizes (16–147 nm) by varying the ratio of citrate to gold [54]. In 1994, Brust set another milestone with the synthesis of thiol-stabilized gold nanoparticles by his two-phase-synthesis [21]. One year earlier, the possibility to stabilize gold nanoparticles with thiols was reported by Mulvaney and Giersig [151]. The method is similar to Faraday's synthesis: $AuCl_4^-$ is transferred to toluene by a phase transfer reagent. In the organic phase, $AuCl_4^-$ is reduced by $NaBH_4$ which is immediately seen as the color of the organic phase changes from orange to brown indicating the formation of gold nanoparticles. During the synthesis, the particles are "covered" with a shell of dodecanethiol ligands. The Brust–Schiffrin method allows the synthesis of thermally stable and air-stable gold nanoparticles. The particles show reduced polydispersity and the size can be controlled from 1.5 to 5.2 nm. The work opened the way for functionalization of gold nanoparticles with a variety of thiol ligands [30, 88]. An even narrower size distribution than with alkanethiol should be achievable by the stabilization of Au nanoparticles by dendrons [112].

Another very useful method for the synthesis of nanoparticles is the seeding growth method. It is based on a step-by-step enlargement of before grown particles ("seeds"). Therewith, various sizes with narrow size distribution were synthesized. Gold seed particles of 3 or 12 nm size, respectively, were used to prepare 20–100 nm Au particles by the reduction with citrate, yielding good monodispersity. The use of NH_2OH as reducing agent was tested and resulted in spheres and rods [19]. Jana et al. found that for higher concentrations of seeds, the nanoparticle growth is better controlled. It is also necessary to add the reducing agent slowly to the solution because otherwise the formation of more seeds is promoted instead of growth of the seeds [97]. The method also works on surfaces where the seeds are immobilized [141]. When Au particle monolayers (immobilized on silane-modified glass) are immersed in a growth solution containing Au^+ and NH_2OH, conductive Au films are generated [18]. Currently, such solution-based generated surfaces were tested for

extremely sensitive protein bioassay using surface-enhanced Raman spectroscopy (SERS) [199].

Willner and coworkers introduced an enzyme-coupled process to enlarge Au nanoparticles. The reducing agent, H_2O_2, is synthesized by glucose oxidase in the presence of glucose and O_2. This process has potential application as glucose biosensor [228].

2.1.2 Silver Nanoparticles

In principle, the synthesis of silver nanoparticles can be carried out by the same methods mentioned for gold nanoparticles. The citrate method introduced for gold nanoparticles by Turkevich [207] can be adopted when $AuCl_4^-$ is substituted by a silver salt, i.e., silver nitrate [1, 147]. The method is considered to work in principle, but with less control over size and shape distribution [130]. The size of the particles was about 35 nm with a broad size distribution. For more details regarding the growth stages of silver and even gold nanoparticles, see Abid [1]. Utilization of $NaBH_4$ as reducing agent resulted in ca. 6 nm particles with a narrow size distribution. TEM measurements confirmed spherical particles but no aggregates or rods [130]. Moreover, a method where EDTA is used as the reducing agent is applied which yielded 20 nm silver particles [91]. The size distribution was even narrower than with $NaBH_4$, but there was no size control by changing the concentrations of the reactants [108].

In addition, an analogous method to the two-phase reduction method developed by Brust and Schiffrin [21] has also been reported for the preparation of Ag particles [115].

The seeding method as described before can be performed using NH_4OH as reducing agent to deposit silver salt from solution to the silver seeds. With this method, particles with well-defined size and shape can be synthesized.

Beside these methods, the formation of silver particles without addition of reducing agents by irradiation of a silver salt solution with laser light was observed. Here, usually surfactants such as SDS or Tween 20 are added to the solution as stabilizer. When the process is performed without any surfactant, the created particles show a very large size and shape distribution and tend to aggregate quickly. Smaller particles are synthesized when the concentration of sodium dodecyl sulfate is increased and when the laser power is decreased. A mechanism for the synthesis from "embryonic silver particles" that are rapidly formed and grown in solution was proposed. There is a competition between SDS to cover the surface and the particle growth [3, 133]. Henglein intensively studied the processes involved in particle formation, especially for silver nanoparticles [80].

The photo-induced formation of particles is also used for the synthesis of particles made from other metals than silver [135].

Liz-Marzán and coworkers succeeded in the synthesis of stable spherical Ag nanoparticles by using *N*,*N*-dimethylformamide (DMF) as reducing agent for Ag^+ and poly(*N*-vinyl-2-pyrrolidone) (PVP) as stabilizer [164].

Novel cost-effective method for the silver nanoparticle synthesis is the bioreduction using bacteria, whereas this technique provides particles with nonoptimum size distribution [106].

2.1.3 Platinum, Palladium, and Rhodium Nanoparticles

For the synthesis of platinum nanoparticles, the citrate reduction method is used as well, resulting in a particle size of 2–4 nm that can be further grown by hydrogen treatment [206]. By changing the ratio of reducing agent and metal precursor, 10 nm Pt particles can be achieved [6, 81]. Larger platin nanoparticles by seeding method are described by Bigall [14]. This method enables the synthesis of arbitrary particle sizes between 10 and 100 nm.

Alternatively, one can use organic solvents to reduce metal salts; for example, ethanol was used to prepare Pt, Pd, Au, or Rh nanoparticles in the presence of a protecting polymer, such as PVP [85, 118]. Ethylene glycol or larger polyols are used in the so-called polyol method by Figlarz [50]. This method also allows us to prepare Ag nanowires or nanoprisms (see Sect. 2.2) [186].

In 2004, Panigrahi et al. published the synthesis of Au, Ag, Pt, and Pd nanoparticles by the reduction of metal salts by various sugars [159]. The resulting sizes depend strongly on the sugar that is used. Particle sizes of 1, 3, 10, and 20 nm for Au, Pt, Ag, and Pd were prepared with fructose. With glucose or sucrose, larger particles could be synthesized. Another interesting method for the preparation of platinum particles is the use of dendrimers to stabilize the nanoparticles. With this method, particles with a controlled size well below 5 nm could be prepared [221].

A single-step method to synthesize catalytically active, hydrophobic Pt nanoparticles by the spontaneous reduction of aqueous $PtCl_6^{2-}$ by hexadecylaniline at a liquid–liquid interface was published in 2002 by Mandal et al. [137].

Beyond, hydrogen can be used as reducer for the synthesis of Pt [81]. So, a Pt(II) solution can be reduced by hydrogen in the presence or absence of stabilizing sodium citrate and/or sodium hydroxide. Using citrate and hydroxide slowed down the reduction but elongated the lifetime of the colloids [83]. A corresponding method is used to prepare Pd nanoparticles with a narrow size distribution [81].

2.1.4 Copper Nanoparticles

For the synthesis of copper nanoparticles, different methods have been reported. The synthesis of well-dispersed copper nanoparticles was achieved by the reduction of aqueous copper chloride solution with $NaBH_4$ in the nonionic water-in-oil microemulsions [170]. Pure metallic Cu nanoparticles can also be synthesized by the reduction of cupric chloride with hydrazine in the aqueous hexadecyltrimethylammonium bromide (CTAB) solution. Thereby, the adjustment of the pH is crucial for the synthesis. The mean diameter of Cu nanoparticles first decreased and then approached a constant with the increase of hydrazine concentration, whereas the

CTAB concentration had no significant influence on the size of Cu nanoparticles [28, 220]. However, at a low concentration of CTAB, the particles display a higher degree of size diversity (particles between 5 and 20 nm). But with higher concentrations of CTAB, a lower degree of size variation (2–10 nm) can be achieved [10]. Copper and copper(I) oxide nanoparticles protected by self-assembled monolayers (SAM) of thiol, carboxyl, and amine functionalities have been prepared by the controlled reduction of aqueous copper salts using Brust synthesis and yielding particles with 4–8 nm diameters [9]. Comparably to silver nanoparticles, copper nanoparticles offer a high antimicrobial effect [8].

2.1.5 Cobalt Nanoparticles

To produce monodisperse magnetic colloids (ferrofluids) of cobalt nanocrystals, Sun and Murray [195] reduced cobalt chloride in the presence of stabilizing agents. The sizes of the particles are ranging from 2 to 11 nm with only 7% SD.

The size and shape-selective synthesis of Co spheres and rods was investigated by Puntes and Krishnan in 2001 [169]. They found that the principles in CdSe particle synthesis also work for Co. A two-surfactants system was used, whereas the first surfactant differentially adsorbs to the nanocrystal faces providing rod formation and the second promotes the monomer exchange for focusing of the size distribution [169].

2.1.6 Nickel Nanoparticles

For the synthesis of Ni nanoparticles also, the reduction with hydrazine in an aqueous solution of cationic surfactants (CTAB/TC12AB) with an appropriate amount of NaOH, a trace of acetone, and elevated temperature was studied. Particles with a mean diameter of 10–36 nm, increasing with increasing nickel chloride concentration or decreasing hydrazine concentration, were prepared [27].

The use of hydrogen as a reducing agent is practicable for Ni nanoparticle as well. The synthesis is carried out in organic solution in the presence of a nonionic surfactant. Particle size analysis showed a distribution of 1–4 nm, the average diameter was 2.1 nm [62].

2.2 Shape

The synthesis of spherical metal nanoparticles (pentagondodecahedra and/or icosahedra) is well understood in general, but the processes leading to the growth of nonspherically shaped nanoparticles are rather complex. All synthesis resulting in

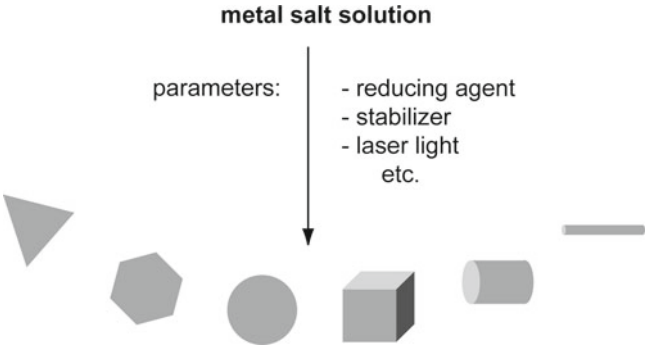

Fig. 1.1 Dependent on various parameters such as type of reducing agent, stabilizers, laser light or others, nanoparticles of different shapes can be realized

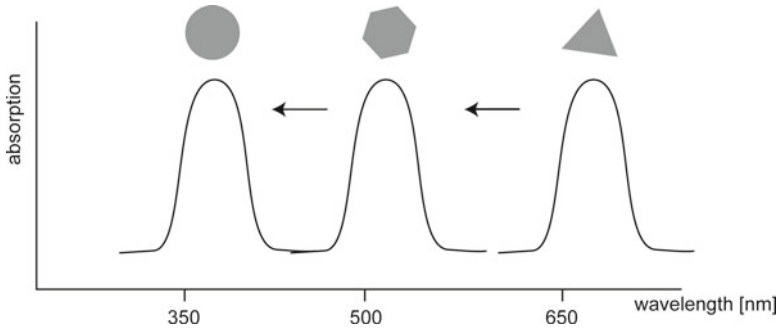

Fig. 1.2 Shift of the surface plasmon resonance during the conversion of triangular-shaped nanoparticles into spheres by heating (Mock 2002)

anisotropic shaped particles are seed-mediated reactions and are dependent on a variety of factors: kinetic parameters, the shape and dimension of the seeds [68], the energy minimum of the crystalline facettes on the seeds, the use of surfactants, and the used reduction agent and silver ions. A systematic overview of the wide range of potential particle shapes for palladium nanoparticles are introduced by the Xia group [222].

Typical surfactant are CTAB [152], poly(sodium styrenesulfonate) (PSSS) [5], Bis(*p*-sulfonatophenyl) phenylphosphine dihydrate dipotassium (BSPP) [101], sodium dodecylsulfate (SDS) [202], bis(2-ethylhexyl) sulfosuccinate (AOT), and PVP [196].

Typical examples for the variety of shapes are: spheres, prisms, rods with different aspect ratios, and cubes with varying edge lengths (Fig. 1.1). In general, beside the size, the shape of a nanoparticle has great influence on the absorption spectrum. This effect is shown in Fig. 1.2 for silver spheres, pentagons, and triangles [145].

2.2.1 Rods

The seeding growth method can be applied for the synthesis of nanorods. For example, 3.5 nm citrate-stabilized Au spheres are used as seeds for the synthesis of Au nanorods with aspect ratios ranging from 4.6 to 18 (with 16 nm short axis each) by varying the ratio of seed to metal salt [23, 99, 152]. Murphy and coworkers improved this method by the substitution of citrate-stabilized Au by CTAB-capped seeds. With this trick, the yield of rod production was increased. The aspect ratios of the rods varied from 1.5 to 10. Ascorbic acid, a milder reducing agent, was used here instead of $NaBH_4$. Absorption measurements showed maxima between 600 and 1,300 nm [98, 154]. Furthermore, experiments were carried out to study the growth processes and the "transformation" of spheres to high aspect ratio rods. It was found that the surfactants applied at the synthesis process play a major role. Two surfactants must be found that differentially adsorb to the nanocrystal faces protecting one face from deposition of further material and another surfactant allowing other faces to grow preferentially [96, 104]. A correlation between both the seed and nanorod diameter has been found. However, on the other hand, the seed diameter could not be proved to correlate to the nanorod length [212]. The purity of the surfactant plays an enormous effect [187]. Changes in the [Br^-] ion amount due to impurity leads to less efficient rod synthesis [58].

In addition, the use of different surfactants and seeding growth has been used also for the synthesis of Co nanorods [169].

Besides, Mokari et al. [146] prepared CdSe nanorods and tetrapods and used Au nanospheres and dithiolhexane to build networks. The Au spheres were attached to the CdSe particles and the interaction of thiols and Au is used to net the CdSe particles with each other [146].

2.2.2 Cubes

Beside nanorods, there were several investigations concerning the formation of nanocubes. Sun and Xia published the preparation of silver nanocubes and hollow gold nanoboxes, respectively [197]. The used method is similar to the so-called polyol method where a metal salt is solved and reduced by ethylene glycol in the presence of PVP. The reaction resulted in slightly truncated nanocubes with edge lengths varying from 70 to 175 nm. By treatment of these nanocubes with gold salt solution, the nanocubes served as templates for the formation of hollow nanoboxes. The silver is oxidized to silver ions and at the same time the gold ions are reduced to gold resulting in highly truncated cubic shape boxes. Murphy and coworkers worked on the synthesis of copper oxide nanocubes of edge lengths of 25–200 nm. The reaction was performed using copper(II) salts, ascorbic acid as reducing agent in the presence of polyethylene glycol (PEG), and sodium hydroxide. By variation of the PEG concentration or the sequence of reactants, the control of edge lengths can be achieved [64, 65]. An overview of the shape control for cubical nanoparticles is given by Tao and coworkers [202].

2.2.3 Prisms

By photo-induced transformation, spheres can be turned into prisms in solution. Jin et al. succeeded in the conversion of 8 nm spheres into prisms with 16 nm thickness and 10–60 nm edge lengths (which transform with time to prisms with 100 nm edge length) by irradiating the solution with light of 350–700 nm wavelengths. The shape transformation is combined with changes in the absorption spectrum [101]. A similar work by Mock showed the progression of plasmon shift due to morphological changes. Triangular-shaped particles are transformed to spherical-like particles by heating. Figure 1.2 shows the absorption spectra of the different shapes produced [145]. Due to different modes of the plasmon excitation, three dominant peaks appear from prisms. Hao and colleagues investigated the plasmon bands more intensely using their prisms with 30, 60, 100, and 150 nm edge lengths. They found in-plane dipole excitation as the red-most plasmon band in the spectrum; the middle band is due to in-plane quadrupole excitation and the bluest band to out-of-plane quadrupole excitation at which the first two are mostly affected by the edge lengths. The spectrum is also sensitive to the thickness and to truncation of the tips of the triangles [73].

Truncated triangles of silver were investigated by Chen et al. using a method similar to the seeding growth method for gold nanorods with ascorbic acid as reducing agent and CTAB as stabilizer. The particles produced had an edge size of ca. 68 nm and a thickness of 24 nm. The degree of truncation was 0.35 [29]. As an alternative, a method has been reported using salicylic acid as reducing agent. The reaction yielded a higher concentration of nanoprisms but produced also hexagonal and spherical-like particles. Furthermore, Figlarz's polyol method allows for the preparation of silver nanowires or nanoprisms, respectively, by the reduction of $AgNO_3$ with ethylene glycol in the presence of PVP [198]. The synthesis of silver triangles using the surfactant PSSS was evaluated by Aherne et al. This method results particles with arbitrary localized surface plasmon resonance in visible spectral range [5]. UV-light modulation of triangles to adjusted plasmon peaks was described by Zhang et al. [230].

2.2.4 Tetrahedron/Octahedron

Experiments with silver, platinum, and copper showed the formation of tetrahedral and/or octahedral structures. In the polyol synthesis of silver nanoparticles using trace amounts of sodium chloride and oxygen, tetrahedrons are produced besides truncated cubes. The dimensions of the particles can be controlled from 20 to 80 nm [216, 217]. The same group also investigated the formation of Pt tetrahedron using basically the same way of synthesis. By increasing the molar ratio between $NaNO_3$ and H_2PtCl_6 to 11, the shape of the synthesized particles turned from irregular spheroids to tetrahedra and octahedra with well-defined facets [84]. Already in 1996, a publication showed the shape-controlled synthesis of colloidal Pt nanoparticles. Several shapes (and sizes) were observed: tetrahedra, cubes, irregular prisms, icosahedra, and cubo-octahedra. The morphology was dependent on the ratio of the capping polymer to the platinum concentration [6].

He et al. published the synthesis of octahedrally shaped Cu_2O particles by the reduction of copper nitrate in Triton X-100 water-in-oil (w/o) microemulsions by gamma-irradiation with average edge lengths ranging from 45 to 95 nm as a function of the dose rate [79].

2.2.5 Nanodiscs

Again, the size is controlled by adjusting the involved reagents and the plasmon resonance modes are different from that of spheres [134]. Nanodiscs of 9 nm thickness and 36 nm diameter were synthesized using SiO_2 particles as templates [73].

2.2.6 Multipods and Nanostars

In the next paragraph, more particular structures are discussed as examples for more complex morphologies.

The first structure is called multipods. The particles show a star-like structure but only with three arms. The plasmon bands in the absorption spectra are sensitive to the length and sharpness of the arms. There is less influence of the thickness and total size [73]. Milliron and coworkers published the preparation of even more complex structures. They demonstrated the synthesis of inorganically coupled colloidal quantum dots and rods (CdTe and CdSe), connected epitaxially at branched and linear junctions within single nanocrystals (ZnS). The advantage of this system is the possibility to tune the properties of each component and the nature of their interactions. The arrangement in 3D is achieved in well-defined angles and distances [143].

Nanostars exhibit hot spots on their arm tips with well-defined geometry [74], these structures represent excellent enhancers for Raman spectroscopic applications (SERS) [89].

2.2.7 Nano Dumbells and Dog Bones

Besides the aspect ratio, also the relation between volume and the shape is a dominant factor in the spectral behavior of plasmonic nanoparticles. Outbreaks and overgrowth of rod-like nanoparticles to dumbbells [69] and dog bones results in interesting fine-adjustment of the LSPR band [224].

2.3 Nanoshells

Another important development demonstrates the so-called nanoshells. In principle, these structures are prepared by covering dielectric nanoparticles (i.e., SiO_2) with a metal (i.e., gold). Thereafter, the core can be dissolved resulting in a hollow nanoshell.

First calculations were done by Aden and Kerker [4] and continued by Neeves and Birnboim [153]. Besides, Halas and coworkers have been pioneers in practical work in this field. The synthesis of the nanoshells is carried out by decorating the silica particle template with small Au colloids followed by the electroless deposition of gold to build a nearly continuous shell. The minimal shell thickness achievable is ca. 5 nm [71, 215]. The plasmon band in the absorption spectrum shifts quite sensitively as a function of the shell thickness. The plasmon resonance of the nanoshells can easily be positioned in the near IR (800–1,300 nm) by variation of the shell thickness. The absorption of biological matter in the near IR is very low which opens the way to several biological applications [16, 72]. Graf et al. propose silica-Au nanoparticles for in various photonic applications [66]. Investigations concerning the shell showed a pinhole structure which is essential for the etching process. The small holes influence the plasmon band not very strong because their size is quite small (2–5 nm) compared to the total particle size (36 nm) [73].

2.4 Fabrication of Nanoparticle Arrays on Surfaces

E-beam lithography can be applied for the synthesis of nanoparticles on surfaces. This top-down nanofabrication method is expensive and serial (disadvantage) but enables for the preparation of ordered two-dimensional arrays of particles all showing the same size, shape, and defined particle-to-particle distance. The last point represents a key advantage of this approach: The nanostructures can be positioned with a high precision regarding both neighboring particles as well as a technical surrounding such as on a chip surface. Aussenegg and coworkers performed pioneering work in this field [39, 63, 173]. They investigated the influence of particle spacing, polarization direction dependence, shape effects due to variation of the aspect ratio of used ellipses, and the possibility to spectrally store data by a special arrangement of the ellipses.

As already mentioned, spheres lead to one plasmon band in the absorption spectrum independent from the direction of polarization. In contrast, ellipses are reacting differently when irradiated with different polarizations: they show a blue resonance when the polarization is orthogonal, but a red peak when the polarization is parallel to the long axis. When the aspect ratio is increased, the peak for parallel polarization is red-shifted. Because the short axis is not varied in the experiments, there was no effect for the orthogonal polarization-dependent peak [63]. The effects caused by the polarization direction-dependent illumination are proposed to be useful for data storage. The arrangement of one, two, or three elliptically shaped particles with defined orientation to each other shows three different possible answers by interaction with light. By varying the polarization direction, it is possible to direct arrangements only in blue or only in red or even in both regimes, always dependent on the orientation of one or more particles in the arrangement relative to the light [39]. Decreasing the interparticle distance but leaving the aspect ratio constant, the plasmon resonance is shifted to red for a polarization direction parallel to

the long axis of the particles. On the other hand, a shift to shorter wavelengths was detected for orthogonal polarization [173, 194].

Experimental and theoretical investigations of 1D arrangements of nanoparticles were also performed. Standard e-beam lithography was used for the formation of such particle chains consisting of elliptically shaped particles with an aspect ratio of 1.4 and 150 nm center-to-center spacing. The polarization direction was chosen parallel to the chains. The plasmon resonance peak is significantly red-shifted compared to the SPR band of a single Au nanoparticle [212].

An alternative method for the production of ordered nanostructures was proposed by Van Duyne and coworkers. Therefore, polystyrene nanosphere monolayers were immobilized on glass substrates serving as a physical masc. Thereafter, gold or silver was deposited onto the substrate followed by the removal of the polystyrene particles leaving behind truncated tetrahedral nanostructures of geometries defined by the size of the polystyrene particles and the amount of deposited metal [77, 100].

Another interesting approach was reported by Alivisatos and colleagues. They produced arrays of nanoparticles and more complex structures such as nanotetrapods by evaporating a nanoparticle solution from the substrate. Hereby, the basis of the assembly mechanism is the interfacial capillary force present during the evaporation [34].

2.5 Methods for Size Reduction

Another top-down fabrication approach is based on interaction of light. Gold nanoparticles in the lower nanometer range can be fabricated by laser ablation (wavelength 1,064 nm) of larger particles. Thereby, irradiation at 532 nm (second harmonic) of 8 nm particles resulted in size reduction. The average diameter decreases with laser fluence (6.2, 5.2, and 4.1 nm with 280, 560, and 840 mJ/pulse cm^2). Larger particles are fragmented by irradiation, whereas smaller particles grow by attracting fragments from the solution. By this process, the size distribution is narrowed indicated by narrowing of the width of the plasmon band [133].

The same goal was followed by Takami and colleagues by irradiating 20 or 50 nm nanoparticles with laser light. The size distribution is again narrowed. A minimal diameter of 10 nm was found even at very high radiation. But laser treatment can also cause shape transformation due to particle heating and subsequent melting of the particles resulting in thermodynamically stable spherically shaped particles. Calculations of the particle temperature showed a heating of up to 2,500 K [200].

2.6 Methods for Size Separation

Hwang and coworkers suggested capillary electrophoresis for size separation. They showed experimentally the separation of polystyrene (PS) or gold particles of

different sizes. It was also possible to distinguish between PS and gold particles of the same size [92]. Alivisatos and coworkers used gel electrophoresis for the separation of gold nanoparticles functionalized with thiol-capped oligonucleotides (see paragraph modifications) [42, 162].

A very precise method for the determination of particle sizes was developed by Galletto and coworkers. They used the hyperpolarizability of first order to detect the size of particles. Small variations in size show a great difference in polarizability. This method could be an effective alternative to the particle size determination with an external reference [57].

3 Bimetallic Particles

Bimetallic particles are classified into two types: first, particles with homogeneous distribution of the two metals are called alloys, and second, particles with heterogeneous arrangement of the two metals, i.e., the so-called core–shell nanoparticles (Fig. 1.3). In principle, the methods for synthesis are derived from the methods for the preparation of monometallic nanoparticles.

3.1 Bimetallic Alloy Nanoparticles

Alloy nanoparticles are synthesized in solution by simultaneous reduction of the two metals of interest (Fig. 1.3). The transformation of core–shell nanoparticles into alloys is another approach that is discussed later.

In general, alloy particles show one characteristic plasmon band. Because of the homogeneous distribution of the metals, alloy particles have homogeneous optical dielectric constants [150]. The position of the LSPR is determined by the ratio of the two metals used. For example, alloy particles consisting of gold and silver

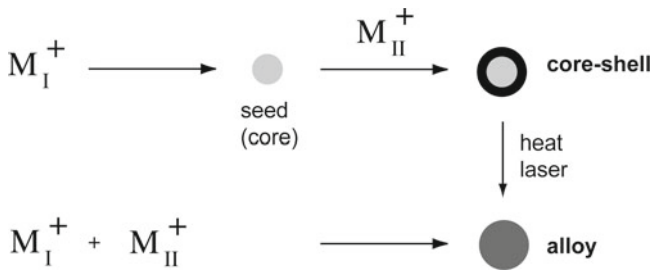

Fig. 1.3 Core–shell particles (*top*) exhibit a defined separation of both metals, whereas alloy particles (*bottom*) consist of a homogeneous mixture. Temperature treatment (e.g., by laser) is known to convert core–shell structures in alloy particles

show a plasmon band ranging between 400 nm (pure silver) and 525 nm (pure gold) [128].

Sànchez-Ramírez et al. synthesized Au/Cu alloys by reducing gold and copper salt solutions with $NaBH_4$ in the presence of PVP as stabilizer. They found a linear law in the position of the LSPR band with the composition of the bimetallic particles as described above [176].

It is possible to prepare a wide variety of alloy particles from several metals. In the early 1990s, scientists found out that alloy nanoparticles provide more catalytic activity than monometallic nanoparticles [205]. Later, the interest for the optical properties has also grown. Alloy nanoparticles of a mixture of gold and silver were also subject matter in many publications. El-Sayed and coworkers synthesized Au/Ag alloys (17–22 nm in size) following a modified protocol by Turkevich [207]. The characterization of the alloys by HRTEM revealed the presence of defects in the homogeneous distribution of the metals such as individual islands of gold and silver within the particles [128]. Alloy synthesis in 2-butanol was applied by Papavassiliou producing 10 nm Au/Ag alloy particles [161].

It is also possible to synthesize alloy particles by laser ablation. Therefore, bulk alloys are treated with laser light in water without any chemical reagents. Lee et al. showed the process for Au–Ag alloy particles with atomic variations of less than 2%. Because of the similar lattice constants, gold and silver are miscible nearly in all proportions. The size distribution could be controlled by the variation of the pulse energy and the time of ablation and the particles could be modified afterwards [125].

3.2 Bimetallic Core–Shell Nanoparticles

Core–shell nanoparticles with inhomogeneous distribution of the metals can be synthesized by the successive reduction of two metal salt solutions. The nanoparticles created during the first reduction process are used as seeds for the second reduction (Figs. 1.3 and 1.4b). Absorption measurements have shown two plasmon bands for these particle structures [150, 151]. The core–shell nanoparticles nearly keep their electronic properties with the electronic band structure of the pure metals. The two bands are only slightly shifted due to interactions between the core and the shell material (Fig. 1.4a).

Noble metals prefer the nonsurface region of the particle [43], but with the addition of a suitable reducing agent, noble metals can also be deposited on less noble metals. To the best of our knowledge, core–shell nanoparticles were synthesized by G. Schmid and colleagues for the first time. He prepared particles with 18 nm Au cores and Pt or Pd shell reaching a total particle size of 35 nm [180]. Then, more and more interest was directed to core–shell particles.

Several bimetallic systems with metals which were already known from monometallic nanoparticle synthesis were used. Lu et al. reported the synthesis of large, monodisperse gold–silver core–shell particles with Ag-like optical properties

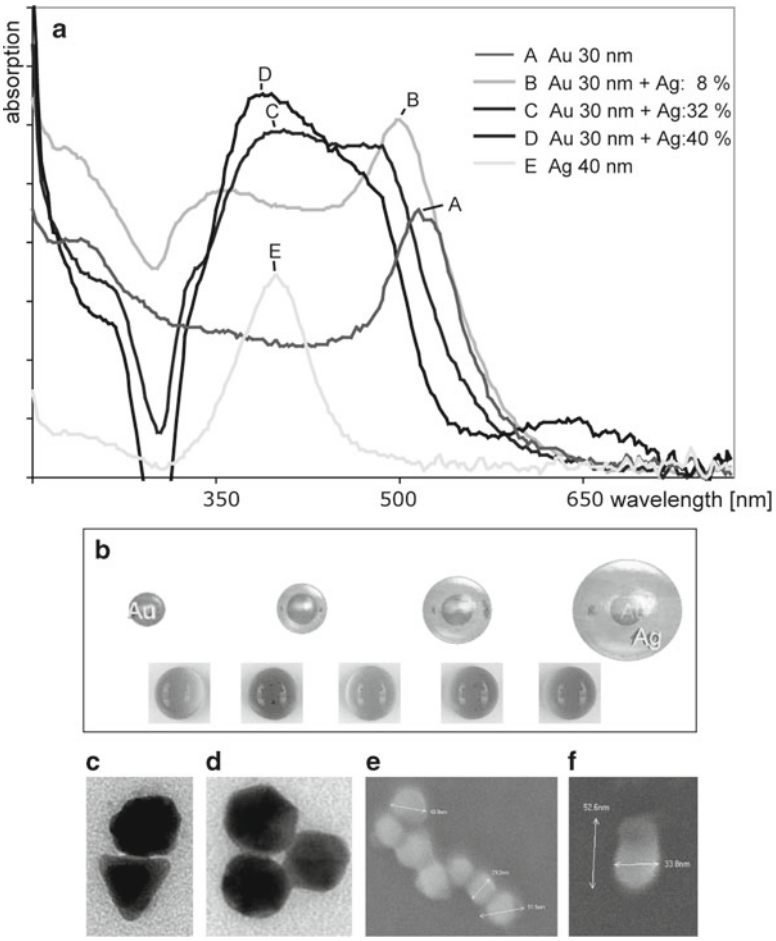

Fig. 1.4 Au-core Ag-shell nanoparticles. (**a**) UV–vis measurements of core–shell particles with increasing silver shell thickness (**b**–**d**) based on addition of different percentages of silver enhancement solution; for comparison the spectra for pure gold (**a**) and pure silver (**e**) are added; (**b**) scheme of enhancement and photographic pictures of droplets of particle solutions; (**c**, **d**) TEM images and (**e, f**) SEM images of Au-core Ag-shell nanoparticles [189]

and ca. 100 nm in size [51]. Soon, an application was found to utilize the core–shell nanoparticles: SERS. First, monometallic silver nanoparticles were applied to enhance the signal from the sample, but also gold–silver bimetallic nanoparticles could be used. Gold seeds are used to deposit silver shells of varying thicknesses (0–100 nm) [136]. The core–shell character of the particles was always revealed from TEM images where brightness differences indicate the metal arrangement (Fig. 1.4c, d). UV–vis absorption spectra show the absorption peaks that reflect a certain composition of the particles. For example, the silver shell in Au–Ag core–shell particles influences on the position of the LSP band of gold. Increasing the Ag

shell thickness results not only in an increase of the absorption signal near 400 nm, but also in a shift of the position of the 520 nm band for gold; i.e., there will occur a blue shift and damping of the LSP signal of gold with increasing Ag content of the particle [3] (Fig. 1.4a).

Besides, the formation of silver core/gold shell particles has been investigated as well. Experiments by Moskovits et al. showed incomplete shell formation only for Au mole fractions below 0.3. Looking more closely to the ultrastructure of the prepared particle, they found a Ag-rich core and a Ag/Au alloy shell whereby the Au fraction grew with increasing Au mole fraction. Furthermore, they theoretically extracted the optical constants from LSP extinction spectra [148]. To suppress the interactions of the two metals in core–shell structures, there is the possibility to separate the core and the shell by an insulating layer of SiO_2. This way, the properties of the core and the shell can be tuned independently and particles with mean total diameters of 120 nm have been synthesized [177].

An interesting method concerning the reducing agent was introduced by Mandal et al. They used UV-switchable so-called "Keggin ions" for the synthesis of Au–Ag core–shell particles [137]. Mirkin's group, the pioneers of nanoparticle modification, also dealt with the modification of bimetallic particles. For alloy structures, the modification was not successful, but the reaction of core–shell particles and thiol-capped DNA resulted in stable particles [24].

Hutter et al. investigated the possibility to connect gold and silver particles together that were synthesized separately in solution. The constructs represent no "real" core–shell particles but it is possible to produce robust gold-encased silver nanoparticles where small (ca. 3 nm) gold particles are attached to ca. 38 nm-sized silver particles. By using larger colloids, chain-like structures are formed [90].

Gold–platinum and gold–palladium are other well-studied systems for bimetallic particle synthesis. Flynn et al. synthesized 11.2 nm gold seeds and deposited Pt with 1–8 mol% [51]. Henglein et al. published the preparation of Pt–Au and Au–Pt nanoparticles by hydrogen reduction and radiolytic techniques. Also, they succeeded in the synthesis of trimetallic particles by the reduction of silver ions by the Au–Pt particles [82]. Moreover, they prepared Pd/Au core–shell particles and trimetallic Pd/Au/Ag particles by Ag deposition on the first mentioned [81].

The experiments of Takatani et al. revealed the importance of the used surfactant for the stabilization of the particles. They tried to synthesize Au/Pt particles with SDS as surfactant, but only monometallic Au (10 nm) and Pt (1 nm) particles were found in the solution. When they used PEG-MS, they achieved a core–shell-like structure. For Au/Pd particles, SDS worked very efficiently as stabilizer reaching 10-nm core–shell particles. The use of PEG-MS resulted also in core–shell formation, but alloys were found in the solution as well and the overall particle size was reduced, whereas the size distribution was broadened [201].

One of the possibilities size distributions to optimize is the use of two-step micro-continuous flow-through method [113]. Such synthesis allows constant residence times and an effective mixing of the components by applying the segmented flow principle. The resulted multi-core–shell nanoparticles offer a narrow size distribution.

3.3 Transformation of Core–Shell into Alloy Nanoparticles

Laser treatment of core–shell nanoparticles can result in the formation of alloy nanoparticles (Fig. 1.3). As mentioned earlier, laser irradiation can cause size reduction and shape changes [56, 105, 200]. Particularly, when laser light is used to irradiate nanoparticles with a resonant wavelength, heat is created in the particles. The temperature can exceed 1,000°C [200]. To the best of our knowledge, the alloying of core–shell particles using ns and ps laser equipment was published first by Hodak et al. in 2000. They found alloying and reshaping of particles after the excitation with a ns laser. When the fluence exceeded a power of over 10 mJ/pulse, fragmentation occurred. Due to more efficient heating, ps excitation led to fragmentation processes already at 4 mJ/pulse fluence [87]. Later, Abid et al. also worked in this field. They used Au_{60}/Ag_{40} core–shell particles with absorption peaks at 410 nm (Ag) and 520 nm (Au) and irradiated them at fluences of 16 or 96 mJ/cm^2, respectively. At a high fluence, the absorption spectra showed only one peak at 510 nm after the laser treatment, indicating the removal of the silver shell and leaving monometallic gold particles. At a low fluence, there was also only one peak detectable in the absorption spectrum but regarding its position (455 nm), it seemed to result from Au/Ag alloy particles. Homogeneous mixing of the two metals is only achieved after numerous pulses because of particle interactions with the environment. That means that the particles do not remain heated long enough to mix within a single pulse because heat leaks to the environment. With each pulse, the particle is heated, partial mixing occurs, and then it cools down again. Using nanosecond laser, less mixing takes place compared to picosecond laser treatment [2]. This method offers an opportunity for the well-defined synthesis of alloy particles by the very selective heating to create new materials with a wide range of composition providing unique optical properties [75].

In addition, we want to mention work where the spontaneous (without any laser excitation) alloying of Au–Ag core–shell nanoparticles was investigated. Shibata et al. have found that the interdiffusion of the two metals was limited to the subinterface layer and depended on the core size and the total particle size. In general, parts of the silver shell do remain. Theoretical calculations confirm the practical results that defects or vacancies at the bimetallic interface enhance the radial migration of the metals [185]. Similarly, spontaneous alloying was also reported for Cu [225] and other metals [166].

4 Nanoparticles and Fluorescence

Novel properties arise from the combination of nanoparticles with fluorescence. First, the so-called quenching effect is used whereby the fluorescence signal decreases with decreasing distance between the fluorophore and a metal particle (Fig. 1.5, left). Second, when the metal particle and the fluorophore are brought

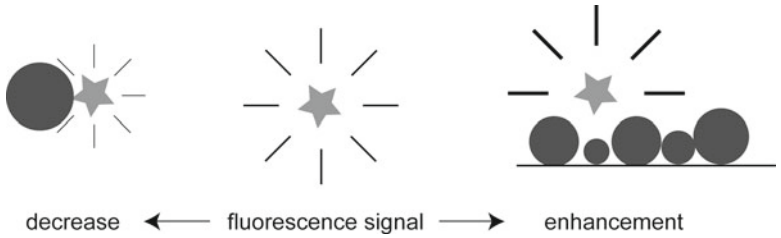

Fig. 1.5 Quenching (*left*) and fluorescence enhancement (*right*) as typical examples for the interactions of fluorescent dyes and metal nanoparticles

together, fluorescence enhancement occurs at certain distances and geometries (Fig. 1.5, right).

4.1 Quenching Effect

Quenching is considered as an energy transfer that occurs when the emission frequency of one molecule (donor) overlaps with the absorption frequency of a second molecule (acceptor). This energy transfer was first observed and investigated by Förster in 1948 [52, 167] and is called Förster resonant energy transfer (FRET). The two interacting molecules can be both fluorophores or a combination of one fluorophore with one metal particle. Here, we only want to discuss fluorophore–nanoparticle systems briefly.

The quenching effect is used in three general approaches: A simple Yes/No answer whether an analyte is present in the test solution, a quantitative analysis of the amount of analyte, or a determination of the distance between donor and acceptor.

Mainly, these tests are DNA-based tests for DNA-analytics or PCR approaches. One approach uses a single-stranded DNA molecule, the so-called molecular beacon that carries both the fluorophore and the metal nanoparticle through covalent attachment [12]. The hairpin loop that is formed to hold the two labels together is opened during the test by hybridization of an analyte to the molecular beacon. Thereby, the distance between the fluorophore and the nanoparticle increases resulting in an increase in fluorescence signal. It is possible to detect SNPs by this principle [42]. The detection of multiple targets in parallel (multiplexing) has been facilitated by the use of several differently colored fluorophores [138, 208]. Furthermore, the identification of retroviruses was shown [209]. Finally, it is possible to monitor nucleic acid detection and PCR quantification in real-time [40].

In addition, the "efficiency" of quenching follows a strict mathematic rule that allows for the determination of the distance between the fluorophore and the metal particle. Förster found that quenching increases with decreasing distance between the two labels following an inverse sixth-order power law. The technique is applied for protein analytics, mainly for monitoring of protein folding/unfolding or the work of the active site of enzymes [127]. FRET in combination with photo-induced electron transfer (PET) even works on the single molecule level.

Instead of "classical" fluorescence molecules, it is possible to use so-called quantum dots. These are nanoparticles made from semiconductor materials (e.g., CdSe) that show high fluorescence and do not suffer from photobleaching, a general problem in fluorescence-labeling techniques. The brightness and photostability of quantum dots allow the detection and observation on the single molecule level [70].

4.2 Fluorescence Enhancement

As described above, quenching normally occurs when a fluorophore and a metal nanoparticle are located very close to each other. But it was described that even fluorescence enhancement can appear when a fluorophore and a metal nanoparticle approach each other [11, 41, 213]. At a distance of ca. 7–10 nm, there exists a local maximum of the fluorescence signal from a fluorophore that is located close to a metal nanoparticle. However, for lower and even higher distances, the fluorescence decreases [103, 121].

The magnitude of the fluorescence enhancement depends on the metal particle, its size, and shape and on the fluorophore type as well. Also the geometry (in the case of multiple metal nanostructures) should influence this effect. There are two pathways upon the interaction of a fluorophore and a metal particle: a radiative and a nonradiative pathway. As mentioned earlier, quenching is due to the absorptive component of the nanoparticle, but fluorescence enhancement, on the other hand, is due to the radiating (scattering) component of the nanoparticle [120]. Therefore, a metallic nanostructure in the vicinity of a fluorophore has great influence on various aspects of the fluorescence emission: the brightness, the lifetime, the absorption and emission spectra, and the effective quantum yield. All these aspect are parts of a causal chain. The starting point is the lifetime of the fluorophore. By decreasing the lifetime, the photostability is increased. Photo-induced destruction can only occur when the molecule is excited. But when the fluorophore is released faster from its excited state, the probability for photobleaching is reduced and the quantum efficiency increases [117, 119, 123].

Lakowicz and coworkers propose the technique for applications in DNA-analytics, immunoassays, for imaging and counting of single molecules, and the control of the flow in microfluidics [121, 122].

Besides these investigations on silvered glass slides, theoretical calculations showed similar facts for fluorophores encased by a metal layer. Enderlein showed theoretically the fluorescence enhancement for polymer beads functionalized with fluorophores that were enclosed by a thin metal layer (5–10 nm of silver or gold) [45].

5 Functionalization of Nanoparticles

Applications of nanoparticles require often a (bio)chemical modification of the particles. This modification can be used to control certain properties of the particle, and/or is needed in order to access the nanoparticle, e.g., for specific binding to

substrates or to other binding partners. In addition, a stabilizing effect due to electrostatic and/or steric reasons can be observed, that is even required in many applications involving higher salt concentrations (e.g., bioanalytics).

5.1 Nanoparticles in Microscopy and Analytics

To the best of our knowledge, the first time when nanoparticles were used for a biological approach was in electron microscopy (TEM) by Palade [158] to detect the transport across the endothelium of blood capillaries. Thereafter, Faulk introduced an immunocolloid method for the electron microscopy based on antibody-modified nanoparticles [48]. Several publications followed describing the detection of human serum albumin [22] or immunglobulins [110, 132], respectively. The detection limit achieved with immunglobulins was lower than pM, and quantitative investigations were possible. Several protocols for the preparation of protein–nanoparticle conjugates (cytochrome *C*, protein A, etc.) are available [76, 108].

Alternatively, DNA can be simply adsorbed on nanoparticles [60] or electrostatic interactions can be used for the binding of charged gold nanoparticles to DNA [226].

5.2 Biotin/Streptavidin

One of the most common biological coupling systems today, the biotin–streptavidin system, was discovered by Chaiet and Wolf in 1964 [26]. The protein streptavidin, found in Streptomycetes, specifically recognizes and strongly binds the small molecule biotin (vitamin H). The strength of the bond is comparable to a covalent linkage and the system was used for biological assays. Biotinylated DNA was detected by a (strept)avidin-modified enzyme in a colorimetric assay [124]. Only 5 years later, the biotin–streptavidin interaction was used for the visualization of sites of nascent DNA synthesis by streptavidin–gold nanoparticle binding to biotinylated nucleotides [86]. Shortly after, Henderson and coworkers reported the labeling of oriented linear DNA molecules with 5-nm gold spheres based on biotin–streptavidin recognition [184].

In another approach, biotinylated RNA of bacterial pathogens was detected by streptavidin-modified gold nanoparticles. The detection system was based on the resonant light scattering of the particles that showed significant lower detection limits (10 fM) than conventional fluorescence systems (500 fM) [53]. The system was used for SERS as well. This method is based on the local signal enhancement for molecules adsorbed at roughened metal surfaces, e.g., silver. The effect is due to the local amplification of the electromagnetic field near rough structures in free electron metals [15]. It was predicted that the detection limit is low enough to investigate single molecules (Kneipp 2002). Moreover, biotinylated silver nanoparticles additionally functionalized with SERS markers were used for the efficient molecular sensing on avidin-modified surfaces [111].

5.3 Thiol Ligands

The modification with thiols especially for gold nanoparticles was extensively investigated during the last two decades. It is based on the high affinity of thiol to gold surfaces [156]. Brust used thiols during the particle synthesis as stabilizer [21]. The disadvantage of the system is that the size of the created thiol-modified nanoparticles is limited to 5 nm. The modification with thiols including dithiols, etc. can be carried out after the synthesis resulting in nearly no limitations regarding the sizes as well [168, 227]. The stabilizing capacity differs for the diverse sulfur ligands, e.g., disulfides are not as good stabilizing agents as thiols. The results of the adsorption of disulfides on gold surfaces show that the binding between gold nanoparticles and thiols is considered as covalent [156]. It was reported by Stellaci and coworkers that thiol (and amine) ligands of variable lengths are organized in highly ordered domains on nanoparticles. This effect was not observed on planar substrates. It has been found that curvature (size dependence) was essential for the formation of the domains. It was proposed to create particles with different "poles" by using different ligands [94]. Furthermore, it was found that thiol ligands affect the electronic behavior of gold nanoparticles. As shown by Zhang and Sham thiols strongly bind to the gold nanoparticle surface and cause charge transfer from the gold to the sulfur ligand [229]. By the utilization of dithiols, a covalent linkage of nanoparticles can be created resulting in aggregation [13, 20].

Mulvaney and coworkers used citrate or alkanethiol stabilized nanoparticles, respectively, for the electrophoretical deposition of highly ordered nanoparticle monolayers [61]. Thereby, the interparticle distance is determined by the chain length of the stabilizer.

For the functionalization of gold nanoparticles with thiol-capped oligonucleotides, see Sect. 5.5.

5.4 Other Ligands

The use of several other ligands has been reported for the stabilization of nanoparticles such as amines [126], carboxyls [139], phosphines (i.e., BSPP) [131, 179, 211], and others. Nanoparticles modified with phosphine ligands (nanogold/undecagold) are commercially available from Nanoprobes, Inc. (http://www.nanoprobes.com).

5.5 Oligonucleotide Ligands

Among all possible modifications, the modification of gold nanoparticles with thiol ligands is the most common and widest used. Since DNA can chemically be modified with thiol groups, it shows potential for the modification of nanoparticles.

In 1996, two groups simultaneously developed a strategy to modify gold nanoparticles with thiol-capped noncomplementary oligonucleotides [7, 144].